JOURNAL OF PHYSIOLOGY AND PHARMACOLOGY 2018, 69, 2
www.jpp.krakow.pl | DOI: 10.26402/jpp.2018.2.11

S. RASCHKA[1], S.K. MORE[2], D. DEVADOSS[2], B. ZENG[1,2], L.A. KUHN[3], M.D. BASSON[2]

# IDENTIFICATION OF POTENTIAL SMALL-MOLECULE PROTEIN-PROTEIN INHIBITORS OF CANCER METASTASIS BY 3D EPITOPE-BASED COMPUTATIONAL SCREENING

[1]Department of Biochemistry and Molecular Biology, Michigan State University, East Lansing, USA; [2]Departments of Surgery, Pathology, and Biomedical Sciences, University of North Dakota, Grand Forks, USA; [3]Departments of Biochemistry and Molecular Biology and Computer Science and Engineering, Michigan State University, East Lansing, USA

In cancer cells exposed to extracellular pressure or shear stress, AKT1-FAK interaction drives focal adhesion kinase (FAK) phosphorylation, leading to force-activated cancer cell adhesion and metastasis. Blocking the AKT1-FAK interaction is therefore an attractive target for cancer therapy, avoiding the side effects of global FAK inhibition. Starting with our previous identification of a short FAK peptide that binds AKT1, we identified a series of small-molecule inhibitor candidates using a novel approach for inhibiting protein-protein interactions. Using a 3D structural fragment of the FAK peptide as the query, millions of drug-like, commercially available molecules were screened to identify a subset mimicking the volume and chemistry of the FAK fragment to test for their ability to block pressure-sensitive FAK phosphorylation by AKT1. Two compounds reduced the stimulation of FAK phosphorylation in response to extracellular pressure in human SW620 colon cancer cells without affecting basal FAK phosphorylation. Thus, using a 3D protein interaction epitope as a novel query for ligand-based virtual screening can successfully identify small-molecules that show promise in modulating cancer cell adhesion and metastasis.

Key words: *adhesion, cancer, ligand-based virtual screening, epitope mimic, focal adhesion kinase, human colon cancer cells, metastasis*

## INTRODUCTION

Most patients with cancer die not of their primary tumor but of metastatic disease (1, 2), yet most cancer pharmacotherapy targets primary tumors and metastasis equivalently. Metastasis is a complex process that requires cells to detach from the primary tumor, access a new space such as the vasculature or lymphatics, and travel to a distant site where they must adhere, invade, and grow (1-5). Physical forces such as extracellular pressure (6) and shear (7) stimulate a complex cytoskeletally-dependent pathway within cancer cells that ultimately increases beta1 integrin heterodimer binding affinity, potentiating metastatic cancer cell adhesion (8, 9). The effect lasts for up to an hour after force activation *in vitro*. Force-activated adhesion occurs in diverse malignancies, including colon and breast adenocarcinoma (10, 11), head and neck squamous cell cancer (12), and sarcoma (13). Cancer cells shed during surgery may be activated by laparoscopic pressures, surgical manipulation, postoperative intra-abdominal pressure increases, or pressure and shear within the lymphatics or circulation. Blocking the pressure-activated pathway that stimulates cancer cell adhesion with high doses of colchicine (14) or siRNA to alpha-actinin-1 (15) improves survival in mouse models of postoperative local tumor recurrence. Blocking this pathway in surgical patients might reduce perioperative tumor dissemination and improve cancer survival.

A key step in the pathway involves AKT1 binding to focal adhesion kinase (FAK), and serine phosphorylation of FAK by AKT1 is required for FAK-Tyr-397 tyrosine autophosphorylation and subsequent FAK activation (16). AKT1-FAK interaction is not generally required for FAK activation by other stimuli (17), while pressure-stimulated signals in macrophages depend upon AKT2, not AKT1 (18). AKT1-FAK interaction therefore seems a appropriate target for intervention to prevent pressure-induced metastasis without inhibiting essential functions. We previously identified a 33-residue peptide within FAK that is required for FAK-AKT1 interaction (19) and reported that adenoviral overexpression of a 7-residue segment prevents AKT1-FAK interaction and consequent force-activation of FAK, ultimately improving tumor-free survival in mice (20).

However, developing peptides as pharmaceuticals is challenging because mammalian digestion and serum proteases inactivate peptides. Blocking protein-protein interactions (PPIs) with drug-like molecules is challenging because PPI interfaces tend to be large and flat, making it hard for small molecules to make sufficient high-affinity contacts with one protein to block binding by its protein partner (21). Consequently, PPI inhibitor discovery through screening by docking often has high false positive and negative rates (22). One promising approach is to experimentally define and mimic an epitope containing several contiguous residues in one of the proteins that accounts for a significant portion of the PPI binding affinity (23). Identifying

the 7-residue FAK peptide described above is an example of this approach.

We propose and test a new method to go a step further to discover drug-like inhibitors of PPIs. Three-dimensional ligand-based screening is typically used to discover new classes of drug-like mimics of a known bioactive small molecule (*e.g.*, a substrate or metabolite). Here, we employ ligand-based screening to discover small molecules that mimic an excised region of a PPI epitope. This technique is powerful because it can equally well be used to find mimics of discontinuous or continuous epitopes. An advantage of ligand-based screening is that knowledge of the molecular interactions between the binding partners is not required; structural knowledge is only required for part of one protein's epitope. Ligand-based screening can match or outperform molecular docking and routinely successfully identify inhibitors (24-26). Another advantage of ligand-based screening is that sources of inaccuracy in docking (e.g., modeling detailed flexibility, electrostatics and solvent contributions) can be avoided by directly identifying mimics of a known bioactive molecule rather than modeling its interactions with a partner. Using this approach, the 7-residue peptide from FAK was used as a query molecule to identify small molecules with drug-like properties that mimic part of the peptide. These candidates were then tested for their ability to block FAK phosphorylation by AKT1 and reduce force-activated cancer cell adhesion.

## MATERIALS AND METHODS

### *Computational screening*

We developed a ligand-based virtual screening protocol (*Fig. 1*) to identify small-molecule mimics of a the FAK peptidyl epitope (LAHPPEE) and a more helical analog (AAHPSEE) that also binds AKT1 (20). For LAHPPEE, we focused on the more rigid LAHPP region (helix-turn) as likely bearing a similar peptidyl structure to intact human FAK (NCBI accession number: NP_722560.1) (27). The 3D atomic coordinates for residues 113-117 (LAHPP) were extracted from the crystal structure of FAK (PDB entry: 2al6) (28). To consider side-chain flexibility, structures reflecting eight favorable alternative positions of Leu were created with backbone-dependent rotamer sampling (29) in PyMOL v. 1.8.2.2 (Schroedinger, LLC); no alternative favorable positions for His were identified. The N- and C-termini of the peptide structure were capped to a neutral state, reflecting their state within intact FAK. To enable chemical matching of polar atoms during screening, partial atomic charges were computed and assigned to the LAHPP structures using molcharge (QUACPAC v. 1.6.3.1; https://www.eyesopen.com /quacpac; OpenEye Scientific Software, Santa Fe, NM) with the AM1BCC force-field (30). Following partial charge assignment, extra protons were removed from the C- and N-terminal nitrogens, and nitrogen charges were set to –0.55, mimicking their state within FAK at physiological pH.

The second query peptide, AAHPSEE (*Fig. 2A*), is a two-site mutant of residues 113-119 in human FAK. In the wild-type structure, the 7-residue peptide consists of a helix terminus followed by a turn. Together they may form a continuous helical epitope upon interaction with AKT1. To test this possibility, the AAHPSEE sequence was designed as a peptide variant with greater helicity, based on the high helical propensity of Ala and the ability of Pro-Ser to form a less bent helix than Pro-Pro. Sequery (31) and Superpositional Structure Assignment (32) were used to evaluate the helicity of sequences matching AAHPSEE in the Protein Data Bank (20, 32, 33). AAHPSEE was subsequently shown to effectively compete with FAK for binding to AKT1 (20). For 3D ligand-based screening, the structure of the AAHPSEE query was built as an alpha-helix in PyMOL (34), with Ser modeled to match the wild-type Pro conformation. The structure was then energy-minimized with YASARA (http://www.yasara.org /minimizationserver.htm) (35), with charges and termini handled as above for LAHPP. These peptide structures were then used as queries to discover the most similar drug-like candidates for testing as potential inhibitors of FAK activation by AKT1 and pressure stimulation of cancer cell adhesion.

For screening, 3D structure files of 10,639,555 commercially available molecules with drug-like properties defined by the Rule of 5 (36) were downloaded from ZINC (http://zinc.docking.org) (37) in MOL2 format. To test the ability of molecules from ZINC to match the known conformation and charge distribution for LAHPP and AAHPSEE peptides, up to 200 favorable 3D conformations were generated for each ZINC molecule using default settings in Omega (version 2.4.1; https://www.eyesopen.com/omega; OpenEye Scientific Software, Santa Fe, NM) (38). To identify structural mimics of the FAK peptide queries, the 3D structures of the drug-like molecular conformers were overlaid on the query molecules using ROCS (version 2.4.6; https://www.eyesopen.com/rocs; OpenEye Scientific Software, Santa Fe, NM) (25). The 3D overlays were assessed by TanimotoCombo scoring, which equally weighs volumetric and chemical similarity. After the

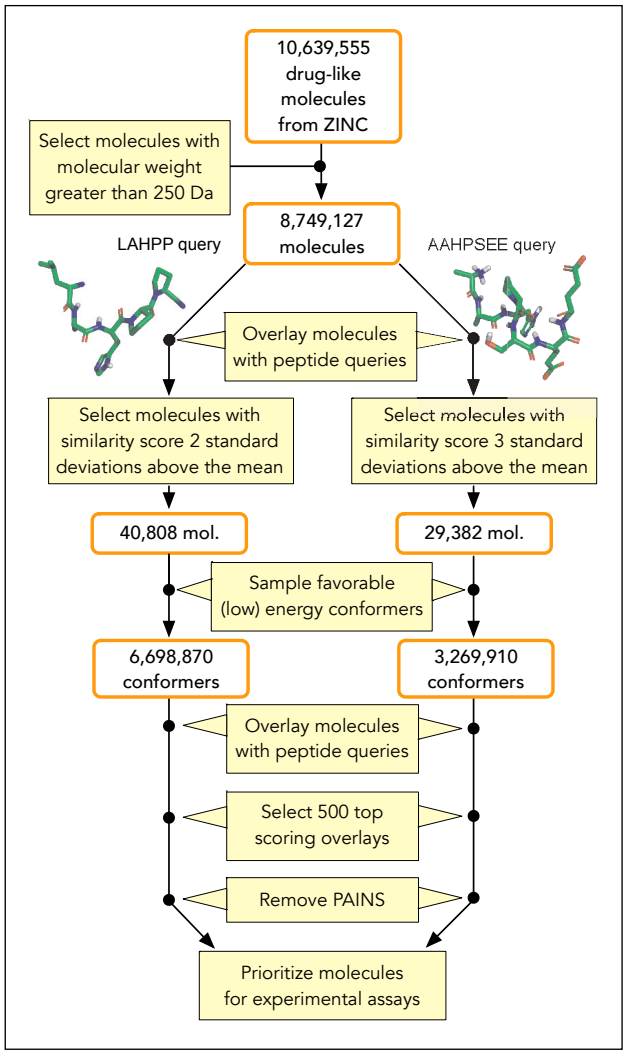


*Fig. 1.* Flowchart outlines 3D ligand-based virtual screening for identifying small-molecule mimics of epitopes from FAK.

top-500 LAHPP and AAHPSEE mimics were identified *via* ligand-based screening, we removed any that were categorized as pan-assay interference compounds, using the PAINS-Remover server (http://cbligand.org/PAINS/) (39).

Final prioritization of molecules for assays was based on visual inspection in PyMOL (34), evaluating the closeness of alignment between the rigid scaffold of the inhibitor candidate and the peptide backbone, and the chemical and volumetric similarity in contiguous, surface-accessible side chains in the peptide. Close analogs of one of the molecules discovered by 3D virtual screening, ZINC04085549 (*Fig. 2C*), were also selected for assays (*Fig. 3*) using the SwissSimilarity webserver (40) (http://www.swisssimilarity.ch) and the http://zinc.docking.org /search/structure search with the ZINC database to find the most shape and chemically similar structures to ZINC04085549. In total, eleven molecules were selected for assay (*Figs. 3* and *4*), representing different structural scaffolds.

*Cells and reagents*

Human SW620 colon cancer cells from the American Tissue Culture Collection were cultured as described (10). Chemical

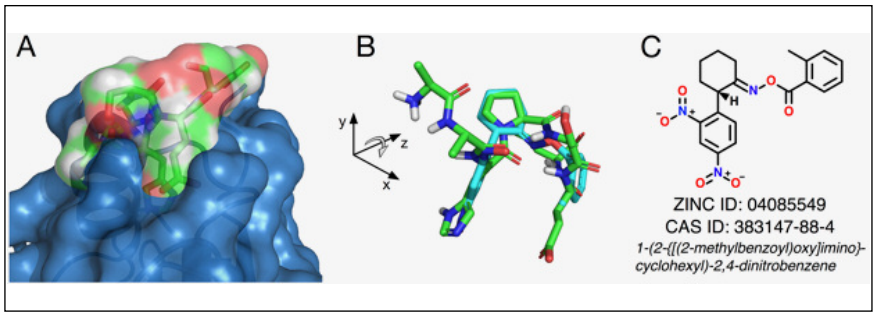


*Fig. 2.* (A) Molecular structure of the AAHPSEE peptidyl epitope used for screening (sticks), shown in place of the wild-type residues 113-119, LAHPPEE, of the FAK FERM domain (PDB entry 2AL6). (B) Structure of AHHPSEE overlaid with ZINC04085549, rotated by ~90º around the z-axis relative to the view in (A). (C) 2D structure of ZINC04085549 with other identifiers.

*Table 1.* Assays of four compounds that mimic the LAHPP epitope in FAK.

| ZINC name | Concentrations studied | Basal FAK-pTyr397 | Pressure stimulation of FAK-pTyr397 | Vendor/Supplier |
|---|---|---|---|---|
| ZINC31501681 | 1 pM – 300 µM | Increased | No further increase | FCH Group (made to order), Chernigov, Ukraine |
| ZINC58264388 | 1 nM – 100 nM | Increased (10–100 nM) | No further increase (10–100 nM) | ENAMINE Ltd., Kiev, Ukraine |
| ZINC40099027 | 10 pM – 10 nM | Increased | No further increase | ENAMINE Ltd., Kiev, Ukraine |
| ZINC25613745 | 1 nM | No change | Maintained | ENAMINE Ltd., Kiev, Ukraine |

*Table 2.* Assays of seven compounds that mimic the active two-site FAK mutant peptide, AAHPSEE.

| ZINC name | Concentrations studies | Basal adhesion | Pressure stimulated adhesion | Vendor/Supplier |
|---|---|---|---|---|
| ZINC04085549 | 10 – 100 µm | Maintained | Blocked ≥ 50 µm | BIONET/Keyorganics, Ltd., Bedford, MA, USA |
| ZINC02457454 | 10 – 200 µm | Maintained | Not inhibited | ChemDiv, Inc., Vistas-M Laboratory Ltd., (Premium), San Diego, USA |
| ZINC04085550 | 50 µm | Maintained | Not inhibited | BIONET/Keyorganics, Ltd., Bedford, MA, USA |
| ZINC12960430 | 50 µm | Maintained | Not inhibited | BIONET/Keyorganics, Ltd., Bedford, MA, USA |
| ZINC4085554 | 10 – 50 µm | Maintained | Blocked ≥ 50 µm | BIONET/Keyorganics, Ltd., Bedford, MA, USA |
| ZINC6241139 | 50 µm | Maintained | Not inhibited | BIONET/Keyorganics, Ltd., Bedford, MA, USA |
| ZINC5816335 | 10 – 50 µm | Maintained | Not inhibited | BIONET/Keyorganics, Ltd., Bedford, MA, USA |

A

ZINC04085549

1-(2-{[(2-methylbenzoyl)oxy]imino}-cyclohexyl)-2,4-dinitrobenzene

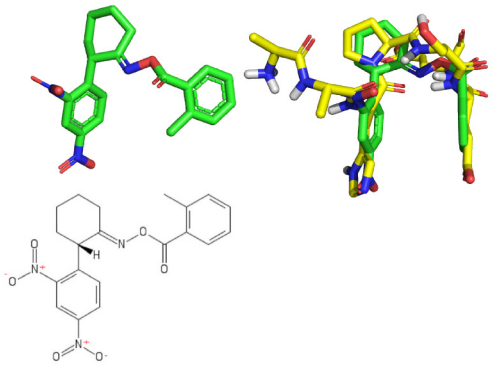

ZINC02457454

N-[1-(cyclopentylcarbamoyl)cyclohexyl]-N-(2-thienylmethyl)benzo[1,3]dioxole-5-carboxamide

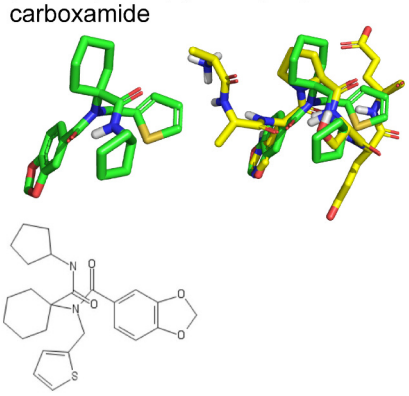

B

ZINC04085550*

1-{2-[(benzoyloxy)imino]cyclohexyl}-2,4-dinitrobenzene

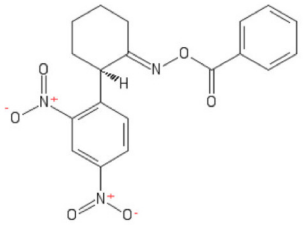

ZINC12960430*

N-[2-(2,4-dinitrophenyl)cyclohexyliden]-N-[(phenylsulfonyl)oxy]amine

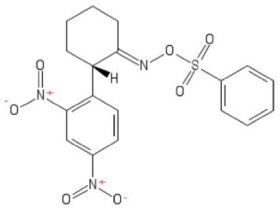

ZINC4085554**

1-(2-{[(4-methoxybenzoyl)oxy]imino}cyclohexyl)-2,4-dinitrobenzene

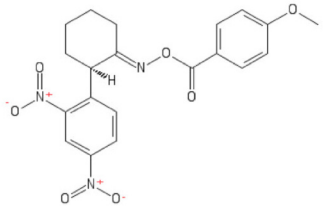

ZINC6241139**

1-(3-{[(anilinocarbonyl)oxy]imino}cyclohexyl)-2,4-dinitrobenzene

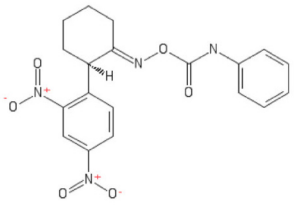

ZINC5816335**

1-(2-{[(cyclopentylcarbonyl)oxy]imino}cyclohexyl)-2,4-dinitrobenzene

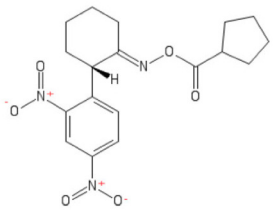

*Fig. 3.* AAHPSEE mimics tested. (A) Two small-molecule mimics selected from ROCS overlays are shown in 2D and 3D representations as well as in a 3D overlay with AAHPSEE. (B) Molecules identified *via* ZINC 2D-Tanimoto similarity search (*) or SwissSimilarity electroshape search (**) using ZINC04085549 from (A) as the query.

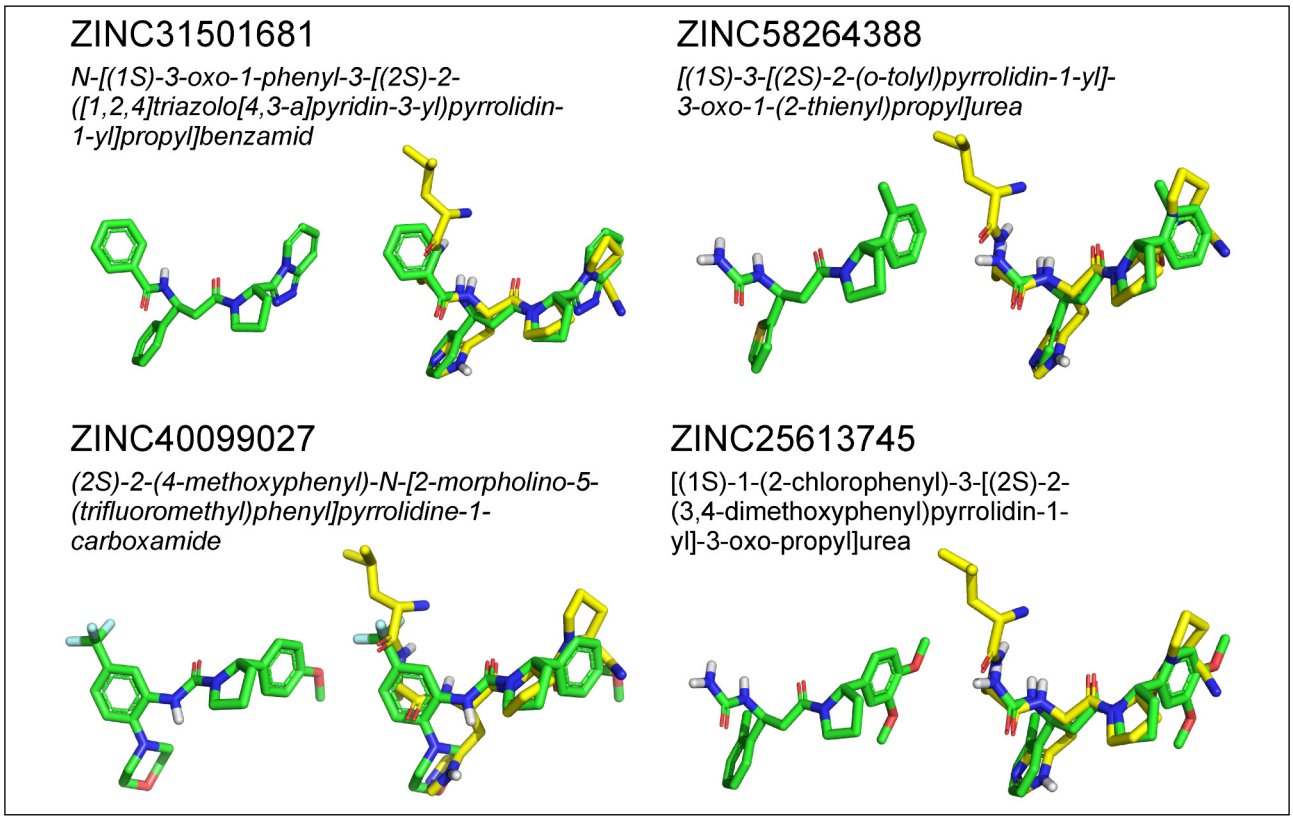


*Fig. 4.* LAHPP mimics assayed. The drug-like mimics overlaid by ROCS are shown with and without the LAHPP query peptide.

compounds from commercial suppliers (*Tables 1* and *2*) were at the highest available purity.

*Extracellular pressure treatment*

Extracellular pressure was increased by 15 mmHg over ambient pressure using a temperature and pressure-controlled box as described (41).

*FAK-Y397 Western blotting*

Cells were maintained at ambient or increased pressure in bacteriologic plastic dishes pacificated with heat-inactivated bovine serum albumin to prevent adhesion and avoid adhesion-associated background FAK activation. Cells were lysed in lysis buffer, resolved by 10% SDS-PAGE, transferred to nitrocellulose and blotted with antibody to Tyr-397-phosphorylated FAK (rabbit monoclonal ab81298, Abcam, San Francisco, CA, USA) and anti-rabbit 680 (LI-COR Inc. Lincoln, NE, USA), before quantitation using Kodak Scientific Imaging Systems 1D, V.3.5.4 (20). Total FAK (Anti-FAK, clone 4.47 Merck, Darmstadt, Germany with secondary anti-mouse 800, LI-COR Inc. Lincoln, NE, USA) served as a loading control. FAK and Tyr-397-phosphorylated FAK Western blots yielded doublets similar to those previously observed by others (42-45). We quantitated both bands together.

*Adhesion assay*

We seeded 50,000 cells/well into 24 well plates precoated with collagen I (Sigma, St. Louis, MO, USA) at 37ºC under ambient or 15 mmHg increased pressure as described (41). After 30 minutes, non-adherent cells were washed away. Adherent cells were stained with MTS (CellTiter 96® AQueous One Solution Cell Proliferation Assay, Madison, WI, USA) and plates were read at 490 nm.

*Statistical analysis*

All assays were performed within linear ranges. Data were normalized against ambient pressure controls treated with DMSO as a vehicle control, represented as X ± SE, and analyzed by t-test seeking 95% confidence.

## RESULTS

The eleven molecules described in the Methods and *Figs. 2*, *3*, and *4* were tested in human SW620 colon cancer cells for their ability to prevent either stimulation of FAK phosphorylation or stimulation of adhesion to collagen.

*FAK phosphorylation studies*

Four structurally similar molecules to the FAK-derived sequence LAHPP (*Table 1*) were evaluated for their ability to prevent FAK activation by 15 mmHg increased extracellular pressure in human SW620 colon cancer cells. FAK-Tyr-397 phosphorylation was measured as an early step in FAK activation, as previously demonstrated in the pressure-activated adhesion pathway (10) and in FAK activation by other stimuli (46, 47). Three molecules, ZINC31501681, ZINC58264388, and ZINC40099027 increased basal FAK-Tyr-397 phosphorylation even at ambient pressure (*Table 1* and *Fig. 3*). Each also prevented a further pressure-induced increase in FAK-Tyr-397 phosphorylation. At 1 nM, ZINC25613745 affected neither basal nor pressure-stimulated FAK-Tyr-397 phosphorylation. *Fig. 5* shows a typical study. The tendency to increase basal FAK

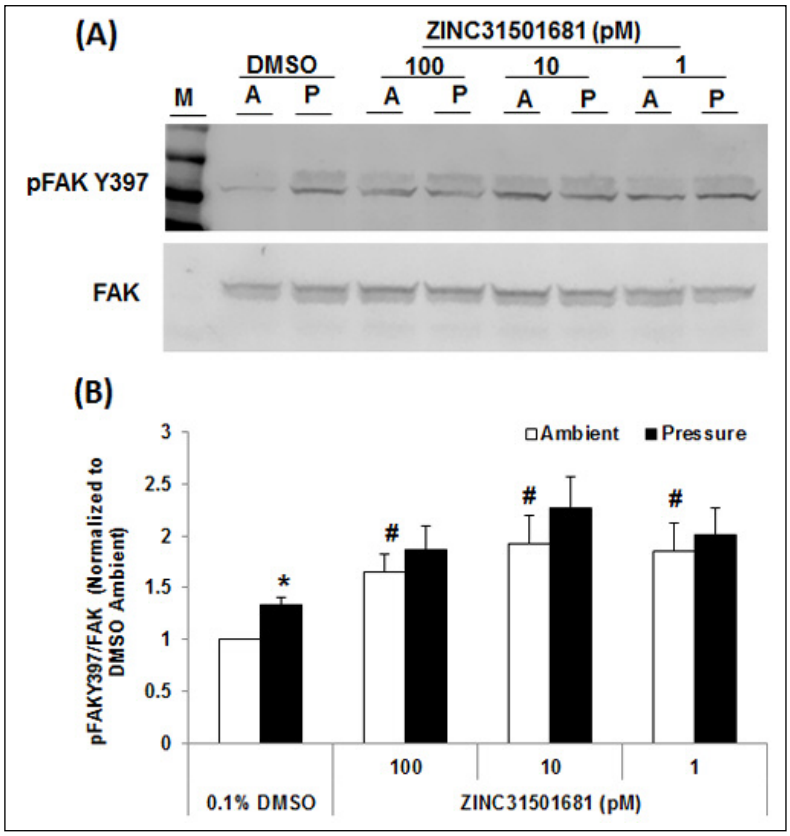


*Fig. 5.* ZINC31501681 enhances the phosphorylation of FAK-Tyr-397 in suspended human SW620 cells at ambient pressure. SW620 cells treated with 0.1% DMSO as a vehicle control or 1-100 pM ZINC31501681 were subjected to ambient (A) or 15 mmHG increased pressure (P) for 30 minutes. A depicts representative western blots probed for FAK-Tyr-397 phosphorylation or total FAK which served as a loading control. B summarizes the densitometric quantitation of pFAKY397/FAK from five independent experiments. (* denotes $P \leq 0.05$ for comparison between 0.1% DMSO ambient and pressure while # denotes $P \leq 0.05$ for comparisons between 0.1% DMSO and 1-100 pM ZINC31501681 at ambient pressure.)

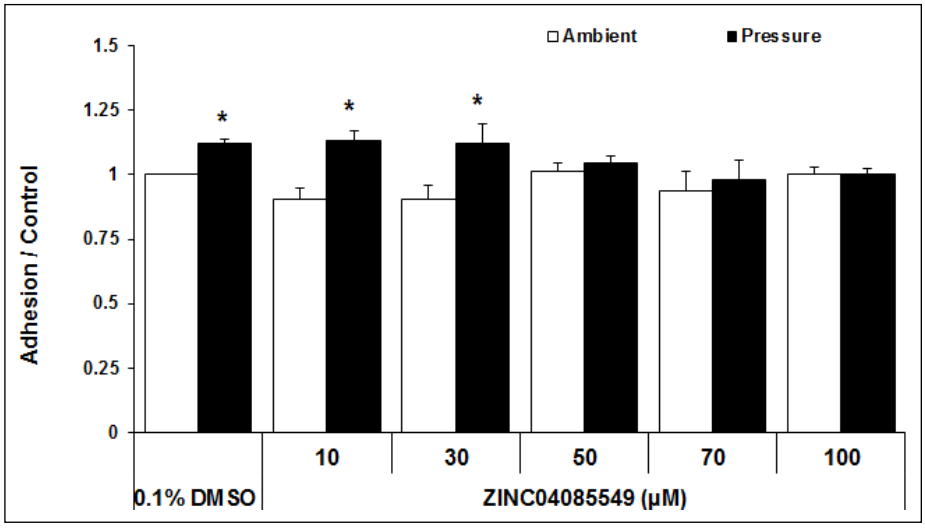


*Fig. 6.* ZINC04085549 blocks stimulation of SW620 cell adhesion to collagen I by increased extracellular pressure. SW620 cells were treated with 0.1% DMSO (vehicle control) or ZINC04085549 at 10 – 100 µM and allowed to adhere to collagen I for 30 minutes at ambient or 15 mmHg increased pressure. (n = 4, *$P \leq 0.05$).

phosphorylation made these LAHPP mimics unattractive for further study, given the goal of blocking FAK activation by phosphorylation.

*Adhesion studies*

We next studied seven molecules that structurally mimic AAHPSEE, including five analogs of ZINC04085549 (*Fig. 3*). These molecules' effects on basal and pressure-stimulated human SW620 colon cancer cell adhesion to collagen I were assayed first. Most molecules had no effect at the concentrations studied (*Table 2*). However, two molecules, ZINC04085549 and ZINC4085554, prevented pressure-stimulated increases in SW620 adhesion without altering basal adhesiveness at ambient pressure (*Fig. 6*).

*Effects of ZINC04085549 on FAK-Tyr-397 phosphorylation*

As one of the promising molecules preventing pressure-stimulated adhesion, ZINC04085549 was further evaluated for the ability to prevent pressure-stimulated FAK-Tyr-397 phosphorylation. At 50 µM, ZINC04085549 prevented pressure-stimulated FAK-Tyr-397 phosphorylation without affecting basal ambient pressure FAK-Tyr-397 phosphorylation (*Fig. 4*).

## DISCUSSION

In vitro high-throughput screening of a large molecular library to identify compounds that block a transiently force-activated pathway would be challenging, because of the time-dependence of

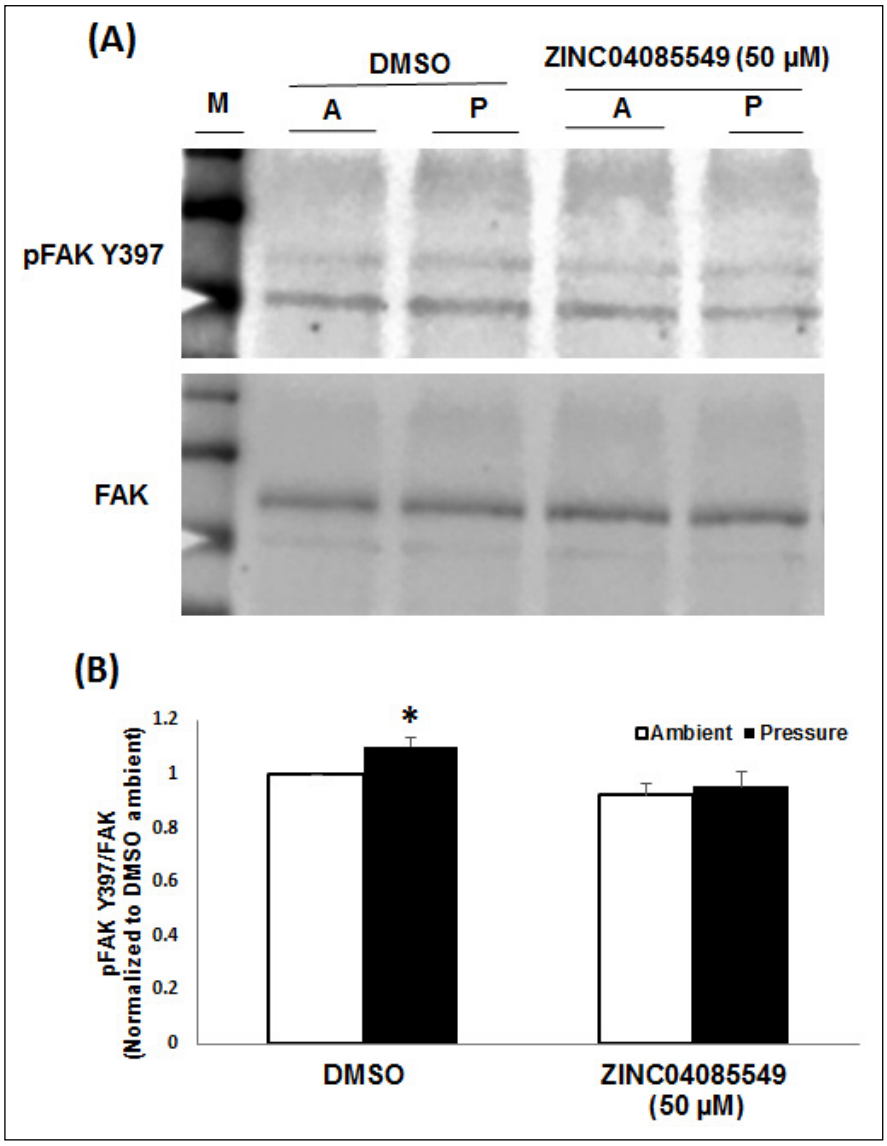


*Fig. 7.* ZINC04085549 blocks pressure-stimulated phosphorylation of FAK-Tyr-397. Suspended SW620 cells treated with 0.1% DMSO (vehicle control) or 50 µM ZINC04085549 were incubated at ambient (A) or 15 mmHg increased pressure (P). A shows representative blots probed for FAK-Tyr-397 phosphorylation and total FAK. B summarizes densitometric quantitation of pFAKY397/FAK from five independent experiments. (*P ≤ 0.05)

the effect and the cost of assaying many purified compounds. Instead, we took advantage of identification of a short FAK peptide involved in AKT1 binding to perform a large-scale computational screen for drug-like molecules mimicking the peptide. By assaying 11 top molecules from the screen, two dinitrobenzene containing molecules, ZINC04085549 and ZINC4085554 (*Fig. 3*), were discovered that block the pressure-induced adhesion of cancer cells. While dinitrobenzene has an unfavorable chemical safety profile (https://www.cdc.gov /niosh/ipcsneng/neng0691.html), nitroglycerin exhibits similar hazards (https://www.cdc.gov/niosh/ipcsneng/neng0186.html), and yet is used to treat angina. Innocuous analogs of these compounds may affect FAK activation similarly. Otherwise, both compounds have drug-like features according to Lipinski's Rule of 5: ≤ 5 H-bond donors, ≤ 10 H-bond acceptors, molecular weight ≤ 500D, and predicted aqueous solubility, as estimated by clogP ≤ 5 (48).

Another important result is that a ligand-based screening technique developed originally to find mimics of small molecules can be effective and efficient in discovering drug-like molecules that mimic PPI epitopes, a much greater challenge. This approach may be applied to other therapeutically relevant PPIs, such as growth factor and immune receptors.

Some candidate molecules activated basal FAK phosphorylation. FAK-397 tyrosine phosphorylation is generally an autophosphorylation event that occurs when FAK dimerizes with itself or other proteins to induce a conformational shift that moves its inhibitory FERM domain and permits autophosphorylation (17). Phosphorylation is maintained until FAK is dephosphorylated by a tyrosine phosphatase such as SHP2 (49) or PTEN (50). This phosphorylation often occurs when FAK is localized in the focal adhesion complex either after integrin-matrix binding (51, 52), after transactivation by other extracellular signals such as muscarinic receptor occupancy (53) or in response to mechanical stimuli such as repetitive deformation or pressure (8, 12, 54). After phosphorylation, FAK may be displaced from the focal adhesion complex into the cytosol where it can be dephosphorylated. How these candidate molecules intervened in this sequence to activate basal FAK awaits study.

In contrast, ZINC04085549 and ZINC4085554 did not affect basal FAK phosphorylation but prevented FAK phosphorylation and adhesion in response to extracellular pressure. Although this level of pressure-induced FAK activation seems modest, it causes substantial survival differences in mouse models of tumor implantation (14).

Future work will test alternative functional groups in ZINC04085549 and ZINC4085554 to enhance their potency and safety. The results show that ligand-based virtual screening can

quickly select from millions of compounds a small number of readily testable, commercially available compounds that are enhanced in activity against pressure-induced cancer cell adhesion, which has been a subtle and intractable problem in cancer therapy.

*Acknowledgments:* We thank OpenEye Scientific Software (Santa Fe, NM) for providing academic licenses for QUACPAC (molcharge), Omega, and ROCS.

Drs. S. Raschka and S.K. More should be considered co-first authors.

Conflict of interests: None declared.

## REFERENCES

1. Chaffer CL, Weinberg RA. A perspective on cancer cell metastasis. *Science* 2011; 331: 1559-1564.
2. Jinnah AH, Zacks BC, Gwam CU, Kerr BA. Emerging and established models of bone metastasis. *Cancers* (*Basel*) 2018; 10: E176. doi: 10.3390/cancers10060176
3. Emenaker NJ, Basson MD. Short chain fatty acids inhibit human (SW1116) colon cancer cell invasion by reducing urokinase plasminogen activator activity and stimulating TIMP-1 and TIMP-2 activities, rather than via MMP modulation. *J Surg Res* 1998; 76: 41-46.
4. Miles FL, Pruitt FL, van Golen KL, Cooper CR. Stepping out of the flow: capillary extravasation in cancer metastasis. *Clin Exp Metastasis* 2008; 25: 305-324.
5. Pingwara R, Witt-Jurkowska K, Ulewicz K, *et al.* Interferon lambda 2 promotes mammary tumor metastasis via angiogenesis extension and stimulation of cancer cell migration. *J Physiol Pharmacol* 2017; 68: 573-583.
6. Thamilselvan V, Basson MD. The role of the cytoskeleton in differentially regulating pressure-mediated effects on malignant colonocyte focal adhesion signaling and cell adhesion. *Carcinogenesis* 2005; 26: 1687-1697.
7. Thamilselvan V, Patel A, van der Voort van Zyp J, Basson MD. Colon cancer cell adhesion in response to Src kinase activation and actin-cytoskeleton by non-laminar shear stress. *J Cell Biochem* 2004; 92: 361-371.
8. Gayer CP, Basson MD. The effects of mechanical forces on intestinal physiology and pathology. *Cell Signal* 2009; 21: 1237-1244.
9. Craig DH, Gayer CP, Schaubert KL, Wei Y, Li J, Laouar Y, *et al.* Increased extracellular pressure enhances cancer cell integrin-binding affinity through phosphorylation of beta1-integrin at threonine 788/789. *Am J Physiol Cell Physiol* 2009; 296: C193-C204.
10. Thamilselvan V, Basson MD. Pressure activates colon cancer cell adhesion by inside-out focal adhesion complex and actin cytoskeletal signaling. *Gastroenterology* 2004; 126: 8-18.
11. Downey C, Alwan K, Thamilselvan V, *et al.* Pressure stimulates breast cancer cell adhesion independently of cell cycle and apoptosis regulatory protein (CARP)-1 regulation of focal adhesion kinase. *Am J Surg* 2006; 192: 631-635.
12. Conway WC, Van der Voort van Zyp J, Thamilselvan V, Walsh MF, Crowe DL, Basson MD. Paxillin modulates squamous cancer cell adhesion and is important in pressure-augmented adhesion. *J Cell Biochem* 2006; 98: 1507-1516.
13. Perry BC, Wang S, Basson MD. Extracellular pressure stimulates adhesion of sarcoma cells via activation of focal adhesion kinase and Akt. *Am J Surg* 2010; 200: 610-614.
14. Craig DH, Owen CR, Conway WC, Walsh MF, Downey C, Basson MD. Colchicine inhibits pressure-induced tumor cell implantation within surgical wounds and enhances tumor-free survival in mice. *J Clin Invest* 2008; 118: 3170-3180.
15. Craig DH, Downey C, Basson MD. SiRNA-mediated reduction of alpha-actinin-1 inhibits pressure-induced murine tumor cell wound implantation and enhances tumor-free survival. *Neoplasia* 2008; 10: 217-222.
16. Wang S, Basson MD. Akt directly regulates focal adhesion kinase through association and serine phosphorylation: implication for pressure-induced colon cancer metastasis. *Am J Physiol Cell Physiol* 2011; 300: C657-C670.
17. Kleinschmidt EG, Schlaepfer DD. Focal adhesion kinase signaling in unexpected places. *Curr Opin Cell Biol* 2017; 45: 24-30.
18. Shiratsuchi H, Basson MD. Akt2, but not Akt1 or Akt3 mediates pressure-stimulated serum-opsonized latex bead phagocytosis through activating mTOR and p70 S6 kinase. *J Cell Biochem* 2007; 102: 353-367.
19. Basson MD, Zeng B, Wang S. The C-terminal region of the focal adhesion kinase F1 domain binds Akt1 and inhibits pressure-induced cell adhesion. *J Physiol Pharmacol* 2017; 68: 375-383.
20. Zeng B, Devadoss D, Wang S, Vomhof-DeKrey EE, Kuhn LA, Basson MD. Inhibition of pressure-activated cancer cell adhesion by FAK-derived peptides. *Oncotarget* 2017; 8: 98051-98067.
21. Arkin MR, Tang Y, Wells JA. Small-molecule inhibitors of protein-protein interactions: progressing toward the reality. *Chem Biol* 2014; 21: 1102-1114.
22. Zahiri J, Bozorgmehr JH, Masoudi-Nejad A. Computational prediction of protein-protein interaction networks: algorithms and resources. *Curr Genomics* 2013; 14: 397-414.
23. London N, Raveh B, Schueler-Furman O. Druggable protein-protein interactions - from hot spots to hot segments. *Curr Opin Chem Biol* 2013; 17: 952-959.
24. McGaughey GB, Sheridan RP, Bayly CI, *et al.* Comparison of topological, shape, and docking methods in virtual screening. *J Chem Inf Model* 2007; 47: 1504-1519.
25. Hawkins PC, Skillman AG, Nicholls A. Comparison of shape-matching and docking as virtual screening tools. *J Med Chem* 2007; 50: 74-82.
26. Raschka S, Scott AM, Liu N, *et al.* Enabling the hypothesis-driven prioritization of ligand candidates in big databases: Screenlamp and its application to GPCR inhibitor discovery for invasive species control. *J Comput Aided Mol Des* 2018; 32: 415-433.
27. Jang B, Jung H, Choi S, Lee YH, Lee ST, Oh ES. Syndecan-2 cytoplasmic domain up-regulates matrix metalloproteinase-7 expression via the protein kinase Cgamma-mediated FAK/ERK signaling pathway in colon cancer. *J Biol Chem* 2017; 292: 16321-16332.
28. Ceccarelli DF, Song HK, Poy F, Schaller MD, Eck MJ. Crystal structure of the FERM domain of focal adhesion kinase. *J Biol Chem* 2006; 281: 252-259.
29. Shapovalov MV, Dunbrack RL. A smoothed backbone-dependent rotamer library for proteins derived from adaptive kernel density estimates and regressions. *Structure* 2011; 19: 844-858.
30. Jakalian A, Jack DB, Bayly CI. Fast, efficient generation of high-quality atomic charges. AM1-BCC model: II. Parameterization and validation. *J Comput Chem* 2002; 23: 1623-1641.
31. Collawn JF, Stangel M, Kuhn LA, *et al.* Transferrin receptor internalization sequence YXRF implicates a tight turn as the structural recognition motif for endocytosis. *Cell* 1990; 63: 1061-1072.
32. Craig L, Sanschagrin PC, Rozek A, Lackie S, Kuhn LA, Scott JK. The role of structure in antibody cross-reactivity

between peptides and folded proteins. *J Mol Biol* 1998; 281: 183-201.
33. Prevelige P, Fasman GD. Chou-Fasman prediction of the secondary structure of proteins. In: Prediction of Protein Structure and the Principles of Protein Conformation, G.D. Fasman (ed.). NewYork, Plenum Press 1989, pp. 391-416.
34. DeLano WL. Pymol: an open-source molecular graphics tool. *CCP4 Newsletter On Protein Crystallography* 2002; 40: 82-92.
35. Krieger E, Darden T, Nabuurs SB, Finkelstein A, Vriend G. Making optimal use of empirical energy functions: force-field parameterization in crystal space. *Proteins* 2004; 57: 678-683.
36. Lipinski C, Lombardo F, BW Dominy PJ Feeney. Experimental and computational approaches to estimate solubility and permeability in drug discovery and development settings. *Adv Drug Deliv Rev* 1997; 23: 3-25.
37. Irwin JJ, Shoichet BK. ZINC - a free database of commercially available compounds for virtual screening. *J Chem Inf Model* 2005; 45: 177-182.
38. Hawkins PC, Nicholls A. Conformer generation with OMEGA: learning from the data set and the analysis of failures. *J Chem Inf Model* 2012; 52: 2919-2936.
39. Baell JB, Holloway GA. New substructure filters for removal of pan assay interference compounds (PAINS) from screening libraries and for their exclusion in bioassays. *J Med Chem* 2010; 53: 2719-2740.
40. Zoete V, Daina A, Bovigny C, Michielin O. SwissSimilarity: a web tool for low to ultra high throughput ligand-based virtual screening. *J Chem Inf Model* 2016; 56: 1399-1404.
41. Basson MD, Yu CF, Herden-Kirchoff O, *et al.* Effects of increased ambient pressure on colon cancer cell adhesion. *J Cell Biochem* 2000; 78: 47-61.
42. McConnell BV, Koto K, Gutierrez-Hartmann A. Nuclear and cytoplasmic LIMK1 enhances human breast cancer progression. *Mol Cancer* 2011; 10: 75. doi: 10.1186/1476-4598-10-75
43. Aflaki E, Balenga NA, Luschnig-Schratl P, *et al.* Impaired Rho GTPase activation abrogates cell polarization and migration in macrophages with defective lipolysis. *Cell Mol Life Sci* 2011; 68: 3933-3947.
44. Das SK, Bhutia SK, Sokhi UK, *et al.* Raf kinase inhibitor RKIP inhibits MDA-9/syntenin-mediated metastasis in melanoma. *Cancer Res* 2012; 72: 6217-6226.
45. Ammoun S, Schmid MC, Zhou L, *et al.* Insulin-like growth factor-binding protein-1 (IGFBP-1) regulates human schwannoma proliferation, adhesion and survival. *Oncogene* 2012; 31: 1710-1722.
46. Schlaepfer DD, Hauck CR, Sieg DJ. Signaling through focal adhesion kinase. *Prog Biophys Mol Biol* 1999; 71: 435-478.
47. Parsons JT. Focal adhesion kinase: the first ten years. *J Cell Sci* 2003; 116: 1409-1416.
48. Lipinski CA, Lombardo F, Dominy BW, Feeney PJ. Experimental and computational approaches to estimate solubility and permeability in drug discovery and development settings. *Adv Drug Deliv Rev* 2001; 46: 3-26.
49. Hartman ZR, Schaller MD, Agazie YM. The tyrosine phosphatase SHP2 regulates focal adhesion kinase to promote EGF-induced lamellipodia persistence and cell migration. *Mol Cancer Res* 2013; 11: 651-664.
50. Tamura M, Gu J, Danen EH, Takino T, Miyamoto S, Yamada KM. PTEN interactions with focal adhesion kinase and suppression of the extracellular matrix-dependent phosphatidylinositol 3-kinase/Akt cell survival pathway. *J Biol Chem* 1999; 274: 20693-20703.
51. Hamadi A, Bouali M, Dontenwill M, Stoeckel H, Takeda K, Ronde P. Regulation of focal adhesion dynamics and disassembly by phosphorylation of FAK at tyrosine 397. *J Cell Sci* 2005; 118: 4415-4425.
52. Walsh MF, Thamilselvan V, Grotelueschen R, Farhana L, Basson M. Absence of adhesion triggers differential FAK and SAPKp38 signals in SW620 human colon cancer cells that may inhibit adhesiveness and lead to cell death. *Cell Physiol Biochem* 2003; 13: 135-146.
53. Calandrella SO, Barrett KE, Keely SJ. Transactivation of the epidermal growth factor receptor mediates muscarinic stimulation of focal adhesion kinase in intestinal epithelial cells. *J Cell Physiol* 2005; 203: 103-110.
54. Thamilselvan V, Craig DH, Basson MD. FAK association with multiple signal proteins mediates pressure-induced colon cancer cell adhesion via a Src-dependent PI3K/Akt pathway. *FASEB J* 2007; 21: 1730-1741.

Received: February 26, 2018
Accepted: April 30, 2018

Authors' address: Prof. Marc D. Basson, University of North Dakota, 1301 North Columbia Road, Grand Forks, ND 58202, USA.
E-mail: Marcbasson@med.und.edu

Dr. Leslie A. Kuhn, Department of Biochemistry and Molecular Biology, 502C Biochemistry Building, 603 Wilson Road, Michigan State University, East Lansing, MI 48824-1319, USA.
E-mail: KuhnL@msu.edu